Chapter 3
Comfort in Buildings

Abstract This chapter reviews basic concepts and terminology of comfort for building's users. Comfort is described from three points of view: i) thermal, ii) visual and iii) indoor air quality. The main comfort indeces which are widely accepted, are presented. Moreover, a comfort analysis which is used to evaluate the performance of the CDdI-CIESOL-ARFRISOL building without the use of any control strategy is done.

3.1 Introduction

Nowadays, energy consumption derived from buildings represents approximately 40% of the total world energy consumption (Atthajariyakul and Leephakpreeda, 2004), and besides, they are also responsible for about 36% of the total worldwide CO_2 emissions. Hence, the integration of renewable energies, energy efficiency and the suitable use of energy inside buildings, are topics that are being widely studied from both scientific and technical points of view (Kolokotsa et al, 2001). However, as people usually spend 80% of their life inside buildings (Kolokotsa et al, 2001), energy efficiency must not endanger users' welfare making it necessary to look for a tradeoff between them. For this reason, control of comfort conditions inside buildings is a problem that is being well analysed, since it has a direct effect on users' productivity and, an indirect effect on energy saving. In general, from users' point of view, a certain environment can be considered comfortable if it is able to provide appropriate thermal comfort, visual comfort and indoor air quality conditions (Dounis and Caraiscos, 2009).

This chapter is organized as follows: the definition of users' comfort from several points of view, thermal comfort, visual comfort and indoor-air quality is presented in Sect. 3.2. Then, a detailed description of the thermal comfort concept and how to estimate it is performed in Sect. 3.3. Moreover, to estimate thermal comfort with the selected index two different approaches are provided appart from the classical one, the first one based on neural networks and the other one based on a polyno-

mial approximation. The main visual comfort indeces are commented in Sect. 3.4 whereas the indoor air quality concept and a new index to estimate it is explained in Sect. 3.5. Section 3.6 is devoted to describing a comfort analysis of a characteristic room of the CDdI-CIESOL-ARFRISOL building. Lastly, the main conclusions which can be inferred from this chapter are discussed in Sect. 3.7.

3.2 Defining Users' Comfort

3.2.1 Thermal Comfort

In accordance with international standards (such as ISO7730 (1994) and ASHRAE55 (1992)) thermal comfort can be defined as: *"That condition of mind which expresses satisfaction with the thermal environment"* (Fanger, 1973). However, this definition can be considered ambiguous, that is, it leaves the meaning of *"condition of mind"* and *"satisfaction"* open, but it emphasizes that comfort is a cognitive process influenced by different kinds of processes, such as, physical, physiological or even psychological. Thermal comfort depends on several circumstances like the place where the person is, the activity that must be carried out in that place, the season of the year, etc. However, according to different studies in this area, although climates, living conditions and cultures differ around the world, the temperature that people choose for comfort under similar conditions of clothing, physical activity, humidity and air velocity is very similar (ASHRAE, 2009).

Many authors have studied the problem of representing and/or computing the thermal comfort condition in a certain environment (Van Hoof, 2008; Orosa, 2009; Sherman, 1985; Wan et al, 2009), and as a result there are some indices and models in the bibliography of this area. Table 3.1 shows a brief review of the different indices which are related to thermal comfort (Taleghani et al, 2013). However, the most extended one is the Predicted Mean Vote (PMV) index, developed by Fanger (Fanger, 1972) during the 70s to guarantee the thermal comfort of humans (Orosa, 2009). In the following sections, the most important indices are explained. More specifically, the selected indices or guidelines explained are those which appear as reference to estimate thermal comfort in recognized standards (ISO7730, 1994) and (ASHRAE55, 1992).

3.2.2 Visual Comfort

In general, the human being receives most information through the sense of sight, and thus, light is a very important element since it allows humans to discern the shape, the colour and the perspective of different objects in a certain environ-

Table 3.1 Chronological development of indices related to thermal comfort. Source: (Taleghani et al, 2013)

Year	Index
1897	Theory of heat transfer
1905	Wet bulb temperature
1914	Katathermometer
1923	Effective temperature
1929	Equivalent temperature
1932	Corrected effective temperature
1937	Operative temperature
1945	Thermal acceptance ratio
1947	Predicted 4-h sweat rate
1948	Resultant temperature
1955	Heat stress index
1957	Wet bulb globe temperature
1957	Oxford index
1957	Discomfort index
1958	Thermal strain index
1960	Cumulative discomfort index
1962	Index of thermal stress
1966	Heat strain index (corrected)
1966	Prediction of heart rate
1970	**Predicted Mean Vote**
1971	New effective temperature
1971	Wet globe temperature
1971	Humid operative temperature
1972	Predicted body core temperature
1972	Skin wettedness
1973	Standard effective temperature
1973	Predicted heart rate
1986	Predicted Mean Vote (modified)
1999	Modified discomfort index
1999	Physiological equivalent temperature
2001	Environmental stress index
2001	Universal thermal climate index
2005	Wet bulb dry temperature

ment (Guasch et al, 2001). Hence, the lighting of a certain indoor environment should satisfy three main tasks (CIBSE, 2002):

- To ensure the safety of people in the environment.
- To facilitate the performance of visual tasks.
- To aid in the creation of an appropriate visual environment.

Therefore, visual comfort can be defined as *"a subjective condition of visual well-being induced by the visual environment"* (12665, 2002). From this definition, it can be inferred that although there is a psychological component in visual comfort sensation, some physical properties of the visual environment can be used

to evaluate it in an objective way (Frontczak and Wargocki, 2011). More specifically, the main parameters which determine visual comfort inside an environment are: luminance distribution, illuminance and its uniformity, glare, colour of light, colour rendering, flicker rate and amount of daylight. The optimal values for these parameters are determined in international research and are published in the international standard UNE EN 12464-1 which makes reference to lighting of indoor work places (12464-1, 2002). As an example, in Table 3.2, the optimal levels for illumination, glare and colour rendering for offices can be observed.

Table 3.2 Recommendations for the lighting for offices. Source: (CIBSE, 2002)

Activity	Maintained illuminance $[lux]$	Limiting glare rating	Minimum colour rendering (R_a)
Filing, copying, etc.	300	19	80
Writing, typing, reading, data processing	500	19	80
Technical drawing	750	16	80
CAD work stations	500	19	80
Conference and meeting rooms	500	19	80
Reception desk	300	22	80
Archives	200	25	80

Furthermore, to achieve suitable visual comfort conditions as a function of the previous parameters, three important elements must be considered: daylight, artificial lighting and shading devices. Therefore, visual comfort conditions inside a certain enclosed area will also depend on the geographical and atmospheric properties of the location where this area is located. In Sect. 3.4, some indeces that allow to quantify visual comfort from illumination, glare and colour rendering points of view are presented.

3.2.3 Indoor Air Quality

There is a relatively new concept in the framework of building use and construction, *"The Sick Building Symptom"*. It can be considered a synonym of poor indoor-air quality, that is, it is defined as the possible appearance of health problems and lack of comfort for the users (Awbi, 2003). Therefore, indoor air quality is defined as a function of the degree in which human necessities are satisfied. Basically, the users of a certain environment demand two things: to perceive fresh air, instead of vitiated, loaded or irritated one, and, to know that the health risk which could derived from breathing that air is depreciable (Castilla et al, 2010a).

Generally, carbon dioxide, CO_2, is the main waste from human respiration. CO_2 concentration is used to estimate the volume of outdoor air intake in order to dilute

overall indoor-air pollution. CO_2-based controls were proposed to maintain adequately low CO_2 levels. Although CO_2 is not the only indoor-air pollutant, other pollutants could be controlled to acceptable low levels as well (Atthajariyakul and Leephakpreeda, 2004). To control CO_2 levels inside a certain environment, the most used technique is ventilation, which can be defined as air supply and/or extraction in a certain environment, establishment or building, in a natural or mechanical form (Hernández, 1994). The main advantage of this CO_2 based demand controlled ventilation is that air ventilation is increased when occupation is high to ensure acceptable indoor-air quality whereas, on the contrary, when occupation is low air ventilation is decreased to save energy (Atthajariyakul and Leephakpreeda, 2004). Moreover, when occupation is high, besides an increase in air ventilation, indoor temperature increases too. Hence the thermal comfort control problem is directly affected, which is logical because it is a multiobjective control problem.

Therefore, in reference to international standards, just as (prEN 13779, 2007; prEN 15251, 2007), indoor-air quality could be classified by CO_2 concentration, since it is the main bioeffluent from human respiration. More specifically, indoor air quality can be classified into four categories, see Table 3.3.

Table 3.3 Basic classification of indoor air quality (IDA) (prEN 13779, 2007)

Category	Description	Typical range [ppm]	Default value [ppm]
IDA 1	High indoor air quality	≤ 400	350
IDA 2	Medium indoor air quality	$400-600$	500
IDA 3	Moderate indoor air quality	$600-1000$	800
IDA 4	Low indoor air quality	>1000	1200

3.3 Thermal Comfort Indeces

3.3.1 PMV Index

The PMV index predicts the mean response (in a statistical sense) regarding thermal sensation of a large group of people exposed to certain thermal conditions for a long time, (IDAE, 2007). The value of the PMV index is a seven-point thermal sensation scale that is shown in Table 3.4. To ensure a thermal comfort situation in a certain environment, different standards recommend to maintain the PMV index at level 0 with a tolerance of ± 0.5 (Liang and Ruxu, 2005).

The PMV index is defined by the six variables that appear in Table 3.5, namely metabolic rate, clothing insulation, air temperature, mean radiant temperature, air velocity and air relative humidity. The acquisition of the major part of these variables is carried out using a simple methodology (Tse and Chan, 2008). Specifically,

Table 3.4 Thermal sensation scale

PMV	Sensation
+3	Hot
+2	Warm
+1	Slightly warm
±0	Neutral
-1	Slightly cool
-2	Cool
-3	Cold

Table 3.5 Variables which define comfort (IDAE, 2007)

Parameter	**Symbol**	**Range**	**Unit**
Metabolic rate	M	0.8 to 4	met (W/m^2)
Clothing insulation	Is_{cl}	0 to 2	clo (m^2 ^{o}C/W)
Indoor air temperature	$T_{a_{in}}$	10 to 30	^{o}C
Mean radiant temperature	T_{mr}	10 to 40	^{o}C
Indoor air velocity	$v_{a_{in}}$	0 to 1	m/s
Air relative humidity	Rh	30 to 70	%

air temperature, air velocity and air humidity are obtained directly through sensors. However, clothing insulation and human activity are variables not easily measurable except in controlled experiments. The main reason is that they depend on the current situation of the users at every instant. The values of both variables can be found in manuals and standards such as (ISO7730, 1994) and (Fanger, 1972). For example, clothing insulation values for a typical office are 1.0 clo[1] and 0.5 clo[1] for winter and summer, respectively, whereas a typical value used for human activity in an office is 1.0 met[2]. Finally, mean radiant temperature (T_{mr} in [^{o}C]), that can be defined as the uniform temperature of an imaginary enclosure in which, radiant heat transfer from the human body equals the radiant heat transfer in the actual nonuniform enclosure (ASHRAE, 2009), can be estimated using different methods:

- From the plane radiant temperature, T_{pr} in [^{o}C], in six opposite directions, weighted according to the projected area factors for a person, as Eq. 3.1. Using this methodology a set of six sensors used exclusively to estimate mean radiant temperature is necessary (ASHRAE55, 1992).

$$T_{mr} = (0.18[T_{pr}(up) + T_{pr}(down)] + 0.22[T_{pr}(right) + T_{pr}(left)] + \\ +0.30[T_{pr}(front) + T_{pr}(back)])/(2[0.18 + 0.22 + 0.30]) \quad (3.1)$$

[1] 1 clo = 0.155 m^2 ^{o}C/W.

[2] 1 met = 58.15 W/m^2.

- From a black globe thermometer, which consists of a hollow sphere usually of 150 *mm* in diameter, coated with flat black paint with a thermocouple build at its centre (ASHRAE, 2009). Thus, the mean radiant temperature can be calculated as a function of the globe temperature, T_g, using Eq. 3.2. More information about how to use the black globe thermometer and how to obtain the mean radiant temperature through the globe temperature can be found in (ASHRAE, 2009; Bedford and Warmer, 1934; Vernon, 1932). With this strategy, only an extra sensor is necessary to estimate mean radiant temperature. Thus, it is a more efficient methodology, in economic terms.

$$T_{mr} = \left((T_g + 273)^4 + \frac{1.10 \times 10^8 v_{a_{in}}^{0.6}}{\varepsilon D^{0.4}} (T_g - T_{a_{in}}) \right)^{\frac{1}{4}} - 273 \tag{3.2}$$

where

  - T_g: globe temperature [°C].
  - $v_{a_{in}}$: air velocity [m/s].
  - $T_{a_{in}}$: air temperature [°C].
  - D: globe diameter [m].
  - ε: emissivity (0.95 for black globe).

3.3.1.1 Classical Approach

The PMV index is based on human thermal sensation which is strongly related to the energy balance of the body when the human body is considered in a heat balance situation, i.e. the heat produced by metabolism equals the net loss of heat, the person is in ideal conditions of comfort and the PMV index is equal to 0. The classical way in which the PMV index can be estimated through the six variables that appear in Table 3.5 was presented in Fanger (1972) and it is shown in Eq. 3.3:

$$PMV = \left(0.303 exp^{-0.036M} + 0.028 \right) L \tag{3.3}$$

In the previous equation, L is the thermal load in the human body (W/m^2), defined as the difference between the internal heat production and the heat loss which occurs when the person is in a thermal situation. Thermal load can be estimated using Eq. 3.4 (Fanger, 1972).

$$
\begin{aligned}
L = {} & (M-W) - 0.0014M(34-T_{a_{in}}) + \\
& - 3.05\times 10^{-3}\left[5733 - 6.99(M-W) - p_{a_{in}}\right] + \\
& - 0.42(M-W-58.15) + \\
& - 1.72\times 10^{-5} M(5867 - p_{a_{in}}) + \\
& - 39.6\times 10^{-9} F_{cl}\left[(T_{cl}+273)^4 - (T_{mr}+273)^4\right] + \\
& - F_{cl} h_c (T_{cl} - T_{a_{in}})
\end{aligned} \tag{3.4}
$$

where

$$
\begin{aligned}
T_{cl} = {} & 35.7 - 0.028(M-W) - 0.155 Is_{cl} \\
& \left[39.6\times 10^{-9} F_{cl}[(T_{cl}+273)^4 - (T_{mr}+273)^4] + F_{cl} h_c (T_{cl} - T_{a_{in}})\right]
\end{aligned} \tag{3.5}
$$

$$
h_c = \begin{cases} 2.38(T_{cl} - T_{a_{in}})^{0.25}, & B > 12.1\sqrt{v_{a_{in}}} \\ 12.1\sqrt{v_{a_{in}}}, & B \leq 12.1\sqrt{v_{a_{in}}} \end{cases} \tag{3.6}
$$

$$
B = 2.38(T_{cl} - T_{a_{in}})^{0.25} \tag{3.7}
$$

$$
F_{cl} = \begin{cases} 1.0 + 0.2 Is_{cl}, & Is_{cl} \leq 0.5\ clo \\ 1.05 + 0.1 Is_{cl}, & Is_{cl} > 0.5\ clo \end{cases} \tag{3.8}
$$

In the previous equations the following variables and parameters not previously defined have been used:

- W: effective mechanical power $[W/m^2]$. The effective mechanical power can be defined as the work carried out by muscles to do a certain task.
- $p_{a_{in}}$: partial water vapour pressure in the air $[Pa]$. The relative humidity, Rh is the ratio, in percentage, between the partial water vapour pressure in the air and the saturation pressure of the water vapour at a certain temperature.
- T_{cl}: clothing surface temperature [°C].
- h_c: convective heat transfer coefficient $[W/(m^2{}^{\circ}\mathrm{C})]$.
- F_{cl}: clothing area factor $[-]$.

At this point, it is important to highlight that, the PMV calculation is not exempt from difficulty. As the reader can observe the clothing surface temperature, T_{cl} must be calculated in a recursive way, see Eq. 3.5. Thus, the usual ways to do this are: i) to give manual values to T_{cl} until both sides of Eq. 3.5 are equal or less than a given tolerance and ii) to use a nonlinear solver. Therefore, the computational effort required by the classical procedure to obtain the PMV index is high. The use of approximated models for this purpose can, on the one hand, reduce the computational cost required to compute the index, allowing its use in real-time control of HVAC systems; and, on the other hand, decrease the size of the network of sensors.

Several works have dealt with approximated thermal models. Artificial Neural Networks (ANN) are used in order to calculate approximated models for the PMV index in Atthajariyakul and Leephakpreeda (2005); Liu et al (2007) or to predict indoor temperature instead of the PMV index, as in Ruano et al (2006). Fuzzy models are also used to approximate the indoor thermal comfort with the aim of controlling it through an HVAC system (Homoda et al, 2012). In the following sections the work presented in (Castilla et al, 2013) is summarized. In this work two approximated models for the PMV index are presented. One of them is based on ANN whereas the other one is a polynomial approximation of such an index.

3.3.1.2 Neural Network Approach

ANN are universal approximators (Cybenko, 1989). The most common type is a static Feed-Forward (FF) configuration that allows to approximate any nonlinear static mapping between input and output variables provided that certain conditions are met. These conditions, regarding the number of nodes of the ANN and the smoothness of the mapping, are often neglected, relying on a final validating step. This is due to the fact that these important factors are, in most cases unknown, leading to an iterative design procedure. Thus, ANN can be considered a black-box model where the model inputs are the number of neurons in the input layer, the model parameters are the number of neurons and the values of interconnection weights, which do not have any physical meaning, in the hidden layers and, lastly, the outputs are the number of neurons in the output layer. A typical ANN scheme with two hidden layers can be observed in Fig. 3.1. The flexibility of ANN comes at a price, not only the number of nodes but also the selection of the weights must be decided by trial and error. In most applications, the iterative design procedure can be tackled using large amounts of data that are split into several sets, some of which are used for training/design and others to validate the solution.

In Atthajariyakul and Leephakpreeda (2005) an FF ANN is used to provide an estimation of Fanger's PMV model. The used variables are air temperature, air wet bulb temperature, globe temperature, air velocity, clothing insulation and human activity. In this way, the authors avoid the need for hygrometers, which are complex and costly and provide a means for low-cost real-time control. The training procedure is based on choosing 2.3×10^5 data points covering the six-dimensional box originated by the Cartesian product of the intervals for each input variable. The intervals are of the form $[v^i_{min},\ v^i_{max}]$ for each variable $i = 1, \cdots, 6$. The structure of the ANN is fixed a priori and consists of two-hidden layers. The number of nodes per layer is also fixed to $6 \times 8 \times 4 \times 1$. The validation is done by comparing the ANN approximation with Fanger's model for an experiment in an office during a working day (from 08h to 17h).

The first issue to be tackled is the ANN structure and, more particularly, the number of hidden layers. According to (Huang et al, 2000), just one hidden layer is needed to approximate any nonlinear smooth map. Using more hidden layers may reduce the number of nodes but that is irrelevant. The important issue is the network

complexity, which is related to the number of parameters which, in turn, is related to the number of connections. The one-hidden layer structure allows for an easy comparison of different sizes with respect to the estimated generalization error. The ANN to be used is thus formed by a hidden layer with n_h nodes with a sigmoidal activation function and one output node with linear characteristic.

The second issue is the election of suitable data-sets in order to train the ANN. The ranges for the variables used to estimate the PMV index, i.e. the metabolic rate (M), the clothing insulation (Is_{cl}), the air temperature ($T_{a_{in}}$), the relative humidity (Rh), the air velocity ($v_{a_{in}}$) and the mean radiant temperature (T_{mr}), are shown in Table 3.6. Two of these variables, M and Is_{cl}, are usually fixed to values that are suggested in international standards (Fanger, 1972; ISO7730, 1994). Thus, a typical election is $M = 1\ met$ and $Is_{cl} = 1\ clo$ or $Is_{cl} = 0.5\ clo$ for winter and summer, respectively, that is, to typical values of an office environment. These values were estimated by Fanger (Fanger, 1972) and were not considered in the developed approximations, since black-box models are used. Therefore, the uncertainty associated to these variables can be associated to the other four variables ($T_{a_{in}}$, Rh, $v_{a_{in}}$, T_{mr}). Thus, the PMV index can be considered only dependent on these four variables.

As was shown in Eqs. 3.1 and 3.2, T_{mr} cannot be obtained directly. On the contrary, it is estimated using either six plane radiant temperature sensors or a globe thermometer, T_g. Both methodologies are valid. Although for the approach developed in this section the last option has been considered. Even though globe temperature range is not specified in the standard, it can be calculated solving Eq. 3.9, which has been obtained from Eq. 3.2, and selecting the most logical roots, i.e. negative and irrational roots are rejected, and positive roots that are out of range also. Thus, it is possible to express the PMV index in terms of T_g instead of T_{mr}.

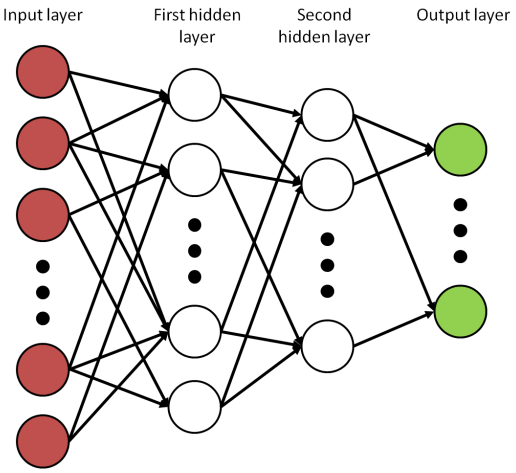

Fig. 3.1 Typical network scheme for a neural network with two hidden layers

$$T_g^4 + (4 \times 273)T_g^3 + (6 \times 273^2)T_g^2 + \left[4 \times 273^3 + \left(\frac{1.10 \times 10^8 v_{a_{in}}^{0.6}}{\varepsilon D^{0.4}}\right)\right] T_g + \\ + \left[273^4 - \left(\frac{1.10 \times 10^8 v_{a_{in}}^{0.6}}{\varepsilon D^{0.4}}\right) T_{a_{in}} - (T_{mr} + 273)^4\right] = 0 \quad (3.9)$$

Table 3.6 Ranges of variables considered to produce GS1 and GS2

Variables	Symbol	Range	Size Step	Unit
Air temperature	$T_{a_{in}}$	10 to 30	1.5	^{o}C
Globe temperature	T_g	10 to 37.25	2	^{o}C
Indoor air velocity	$v_{a_{in}}$	0.06 to 0.5	0.05	m/s
Air relative humidity	Rh	30 to 70	4	%

Moreover, for these four variables ($T_{a_{in}}$, Rh, $v_{a_{in}}$, T_g), subranges included in the ranges presented in Table 3.5 are defined depending on the place where the approximated models will be used. In this case the models are calculated using real data saved during the operation of the CDdI-CIESOL-ARFRISOL bioclimatic building, described in Chap. 2. Once the subranges are defined, see Table 3.6, two global datasets (GS1 for summer and GS2 for winter) each composed of 19404 data points are obtained. The set of points covers the four-dimensional space of the independent variables ($T_{a_{in}}$, Rh, $v_{a_{in}}$, T_g), where all possible combinations among each variable are considered. In addition, each variable changes inside a range delimited by appropriated values for the location of the building and with a fixed step size, see Table 3.6. Once these GS1 and GS2 have been defined, the PMV index can be estimated, using Eqs. 3.3-3.8, for all these combinations.

Following the standard methodology (Reed and Marks, 1999), each GS_X, where $X = 1$ for summer and $X = 2$ for winter, has been split through random sampling without replacement in the following subsets, each composed of 9702 data points:

- A training set (TR_X) for obtaining both, the ANN parameters using a gradient descent algorithm and the polynomial model coefficients defined in the following section by means of a QR factorization (where Q is an orthogonal matrix and R is an upper triangular matrix) with pivoting.
- A testing set (TE_X) for deciding both, the number of nodes in the hidden layer of the ANN and the order of the polynomial model in the case considered in next section.

Although the goodness of the model is validate by the testing set, in order to see the models performance during real days, the models are validated by several real data-sets from the CDdI-CIESOL-ARFRISOL building in order to cover the most usual cases. The obtained models results from these real data-sets are similar in all of them, for this reason a couple of days has been chosen for each season considered, since different PMV models are needed for summer and winter.

Each of these real data-sets corresponds to one day sampling with a sample time of $t_s = 60\ s$, thus, their size is 1440 data points. Therefore, for summer, two data-sets are considered. The first one (VA1a) corresponds to a non-working day, where the real PMV index value is above the comfort band since the HVAC system was disconnected. The second data-set (VA1b) refers to a working day, where the usual occupants were inside the CDdI-CIESOL-ARFRISOL building and the HVAC system was working. Therefore, the real PMV index value for this data-set is inside the comfort band $[-0.5, 0.5]$. In the same manner, for the winter, a working day and a non-working day have been selected as real validation data-sets. Moreover, the first data-set (VA2a) refers to a non-working day where the PMV index value is under the comfort band. For the second data-set (VA2b) the PMV index value is inside it.

Note that, two more data-sets could be chosen for validation. One for the summer, where the real PMV is under the comfort band and another data-set for the winter, where the real PMV is above the comfort band. However, theses cases are unusual in the place where the CDdI-CIESOL-ARFRISOL building is located, Almería, and no real data have been found to be used as data-sets. A summary of the different data-sets used for training, testing and validation models is shown in Table 3.7.

Table 3.7 Data-set description

Name	Use	Origin	Size	Description
TR1	Training	GS1	9702	Summer training set
TE1	Testing	GS1	9702	Summer testing set
VA1a	Validation	Real data	1440	Summer validation set, non-working day
VA1b	Validation	Real data	1440	Summer validation set, working day
TR2	Training	GS2	9702	Winter training set
TE2	Testing	GS2	9702	Winter testing set
VA2a	Validation	Real data	1440	Winter validation set, non-working day
VA2b	Validation	Real data	1440	Winter validation set, working day

Once trained, the goodness of fit of any of the approximations (P) (neural network or polynomial model analysed in next section) is reported using the Root Mean Square (RMS) error, computed over the samples of a particular set S and denoted as $e_S^{RMS}(P)$, thus:

$$e_S^{RMS}(P) = \sqrt{\frac{1}{card(S)} \sum_{i=1}^{card(S)} (y(i) - \hat{y}(i,P))^2} \tag{3.10}$$

where $y(i)$ stands for the correct value of the PMV for element $i \in S$ and $\hat{y}(i,P)$ is the approximation given by the model P for that particular element.

In the training process, input variables can be observed in Table 3.6. Training is performed using a variable-step gradient descent process, namely the MATLAB's implementation of the Levenberg-Marquardt algorithm (Moré, 1978). The *trainlm* function is used for, at most, 30 iterations over the TR. The number of iterations is

reduced to avoid overtraining. The usual procedure when using neural approximations is to normalize the components of the input vector. This is accomplished by subtracting the mean value and dividing it by the standard deviation for each variable. Once trained, the goodness of fit of a particular ANN, (N_{NN}), is reported, using the RMS error, see Eq. 4.18.

An ANN with insufficient nodes may be unable to reproduce the variations of PMV in the data-set. On the other hand, an ANN with more nodes than needed may lead to overtraining and degrade the generalization capabilities.

In order to select the most adequate network size several ANN are trained using data from the TR, with different random initial parameters and with different values of n_h. It is useful to show the relationship between the $e_{TE}^{RMS}(N_{NN})$ and network size n_h. Since the training of the networks relies on random elements, the error $e_{TE}^{RMS}(N_{NN})$ is a random variable, and hence, it is possible to compute its mean and standard deviation. In Fig. 3.2, the mean value for each n_h is plotted with a dark blue solid line and (○) marks for testing sets for the summer, top, and the winter, bottom. The light blue lines above and below represent the mean plus and minus the standard deviation, respectively. For each value of n_h, 50 networks are trained and tested, the experimental mean and standard derivation are taken over these 50 trials for each n_h.

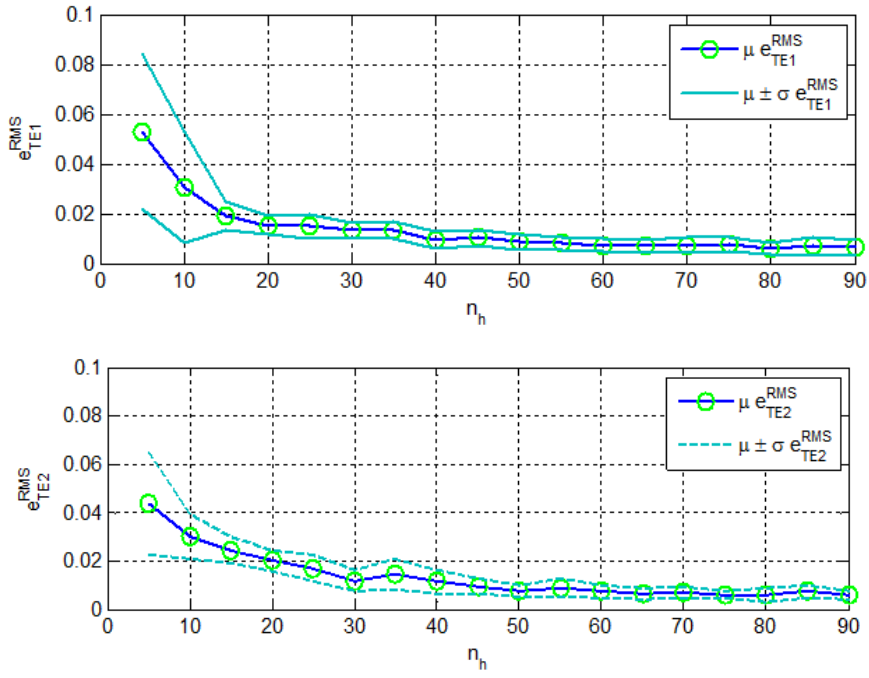

Fig. 3.2 Influence of network size n_h on the mean (μ) and standard error (σ) for the testing set for the summer (top) and the winter (bottom)

The mean value of $e_{TE}^{RMS}(N_{NN})$, for both the summer and the winter sets, does have a clear tendency to decrease with n_h. But it is clear from Fig. 3.2 that for values of $n_h > 50$ the mean value of $e_{TE}^{RMS}(N_{NN})$ is almost constant, that is, the reduction in the mean value is not significant for n_h values greater than 50. Thus, a logical choice is $n_h = 50$, then the number of configurable parameters of the network is $N_p = 50 \times (4+1) + 50 + 1 = 301$. The graphs of Fig. 3.2 indicate that a theoretical mean RMS error about 0.01 is to be expected in both the summer and the winter cases.

In Figs. 3.3 and 3.4, the real and estimated PMV are shown for the four validation data-sets. In addition, the bottom picture of each figure shows the absolute error associated with the four validation data-sets. With respect to the summer results, the neural network model obtains $e_{VA1a}^{RMS} = 0.0117$ and $e_{VA1b}^{RMS} = 0.0079$, for validation data-sets VA1a, VA1b, respectively, see Fig. 3.3. These results are inside the expected range obtained by the testing data-set, and can be considered good enough to use the neural network model when computing the PMV index since in the worst case they have a relative error equal to 4.7%.

On the other hand, with respect to the winter data-sets, the neural network model obtains an RMS error value of $e_{VA2a}^{RMS} = 0.0145$ and $e_{VA2b}^{RMS} = 0.0123$, for validation data-sets VA2a, VA2b, respectively, see Fig. 3.4. As for the summer case, these results are inside the expected range with a relative error in the worst case equal to 5.9%. Moreover, they prove the efficiency of the neural network model to calculate the PMV index with real data from both, non-working and working days.

3.3.1.3 Polynomial Approach

The second approach presented in this section is based on a polynomial approximation for the PMV index. This model has been obtained using a polynomial regression modelling tool, more specifically, the MATLAB *Polyfitn* library (D'Errico, 2012). *Polyfitn* is able to solve the coefficients of a polynomial regression model using classical linear least squares techniques. Several numerical methods have been used to implement the *Polyfitn* library. However, to obtain a more stable solution it is worth highlighting the use of the QR factorization with pivoting for solving the system (D'Errico, 2012). More specifically, within the framework of linear algebra, the QR factorization of a matrix is a decomposition of a certain matrix into a product of an orthogonal matrix Q and an upper triangular matrix R, which are generally used to solve linear least squares problems. In addition, the components of the input vector are normalized before obtaining the polynomial approximation.

As well as in the ANN model, two polynomial models have been obtained, one for each representative season of the year (summer and winter). Models that are ordinary generating functions of a four-dimensional array $a_{i,j,m,z}$, where the indices i, j, m and z belong to the set $C_I = 0, 1, 2, ..., n$ and n is the polynomial degree, are defined by Eq. 3.11.

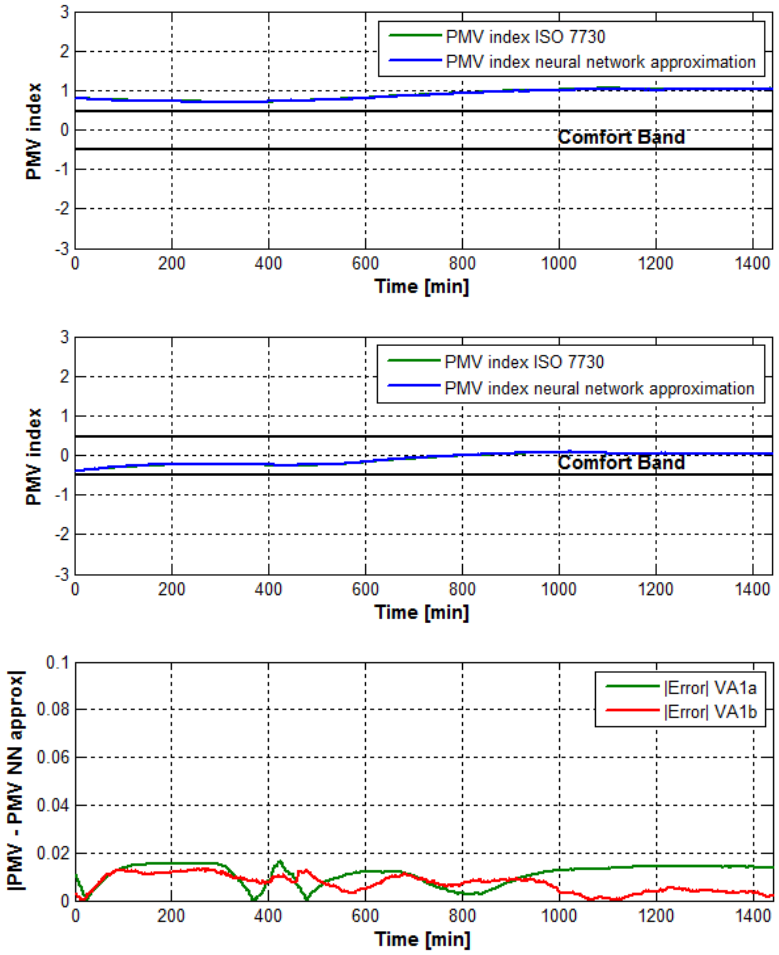

Fig. 3.3 Real PMV index and neural network approximation for the summer data: VA1a (top) and VA1b (middle), and absolute error (real PMV - neural network approximation) for both data sets (bottom)

$$PMV = f(T_{a_{in}}, Rh, v_{a_{in}}, T_g) = \sum_{i,j,m,z \in C_I = \{0,\ldots,n\}}^{R(n+1)} a_{i,j,m,z} (T_{a_{in}}^i Rh^j v_{a_{in}}^m T_g^z) =$$
$$= a_{7,0,0,0} T_{a_{in}}^7 + a_{6,1,0,0} T_{a_{in}}^6 Rh + a_{6,0,1,0} T_{a_{in}}^6 v_{a_{in}} + a_{6,0,0,1} T_{a_{in}}^6 T_g +$$
$$+ a_{6,0,0,0} T_{a_{in}}^6 + a_{5,2,0,0} T_{a_{in}}^5 Rh^2 + \cdots + a_{0,0,0,5} T_g^5 + a_{0,0,0,4} T_g^4 +$$
$$+ a_{0,0,0,3} T_g^3 + a_{0,0,0,2} T_g^2 + a_{0,0,0,1} T_g + a_{0,0,0,0} \quad (3.11)$$

In the previous equation $a_{7,0,0,0}, a_{6,1,0,0}, a_{6,0,1,0}, \cdots, a_{0,0,0,2}, a_{0,0,0,1}, a_{0,0,0,0}$ are constant coefficients obtained by the TR1 for the summer polynomial model, and

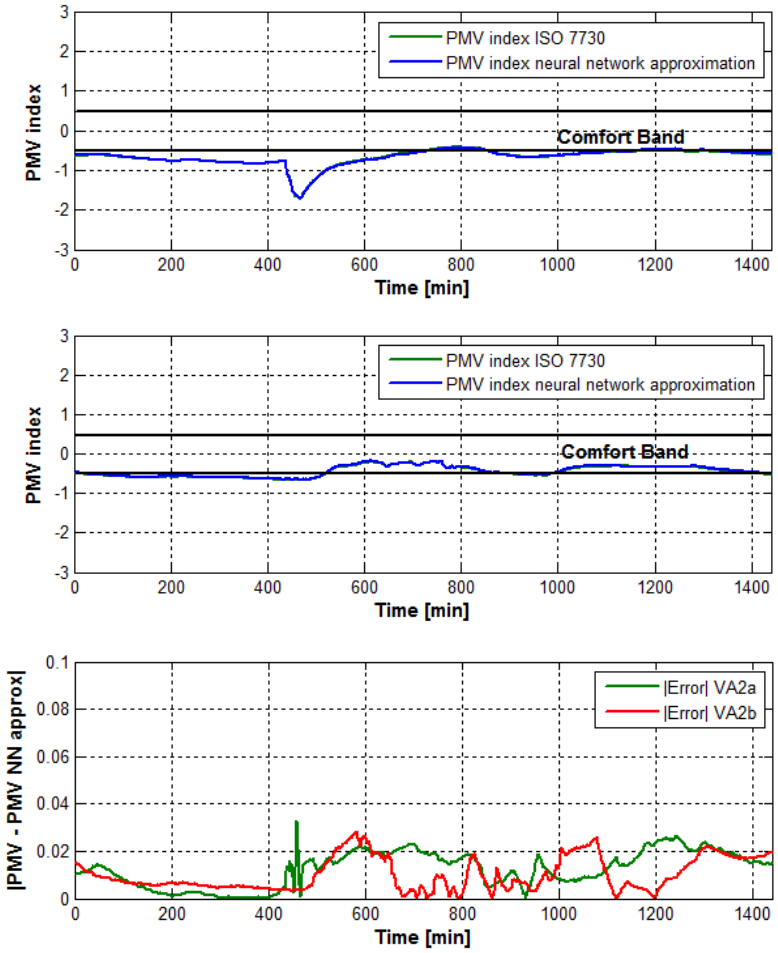

Fig. 3.4 Real PMV index and neural network approximation for the winter data: VA2a (top) and VA2b (middle), and absolute error (real PMV - neural network approximation) for both data sets (bottom)

TR2 for the winter polynomial model. Finally, $R(n+1)$ is a distribution defined by Eq. 3.12.

$$R(k) = \sum_{i=0}^{k} Q(k) \tag{3.12}$$

where

$$Q(k) = Q(k-1) + \sum_{i=0}^{k} i \qquad and\ Q(0) = 0 \tag{3.13}$$

In order to make a fair comparison with the previous models, n has been chosen based on having similar configurable parameters, or degrees of freedom, than the ANN models. Thus, for a seventh degree polynomial, i.e. $n = 7$, the number of terms is equal to 330, which is similar to those obtained in the ANN models. However, the e_S^{RMS} index for testing sets S=TE1 (summer) and S=TE2 (winter) is almost three times bigger than that for ANN models, see Fig. 3.5. Thus, in the polynomial case, a mean RMS error of about 0.03 is to be expected in both summer and winter cases. Lastly, as the number of coefficients is too high, 330, due to lack of space, the polynomial structure is not completely expanded in Eq. 3.11.

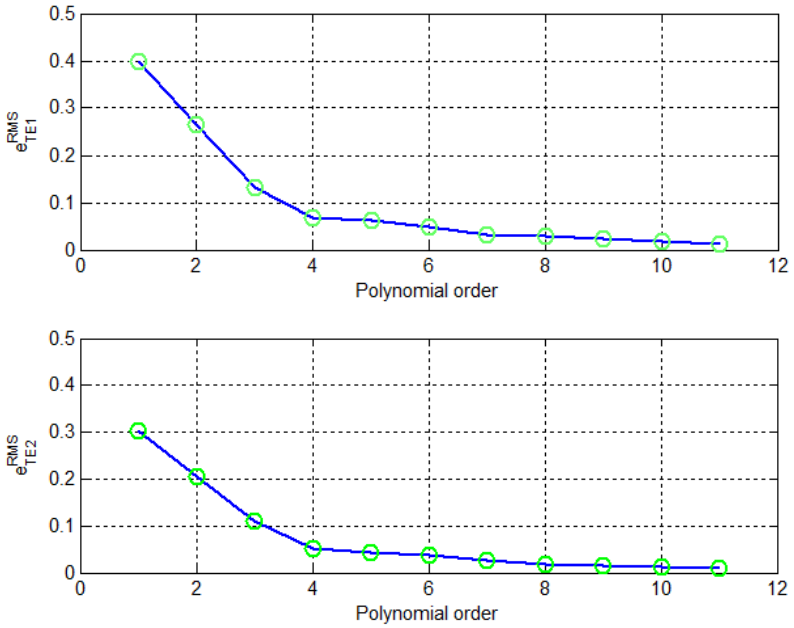

Fig. 3.5 Influence of polynomial degree n on the testing set errors for the summer (top) and the winter (bottom)

As in the case of the ANN models, the polynomial models were tested with the validation data-sets VA1a, VA1b, VA2a and VA2b. From VA1a data-set, a value of $e_{VA1a}^{RMS} = 0.0065$ is obtained, this result is better than expected. See top graph in Fig. 3.6, where an RMS error of about 0.03 was predicted, and even better than the one obtained by the neural network model. On the other hand, with the validation data-set for a summer working day, see the middle graph in Fig. 3.6, the polynomial model obtains $e_{VA1b}^{RMS} = 0.0357$, which is worse than the one from the neural network model, although it is close to the expected value. For the same validation sets, the polynomial approach provides worse results than the neural network approach since, in the worst case, a relative error equal to 8.6% is obtained.

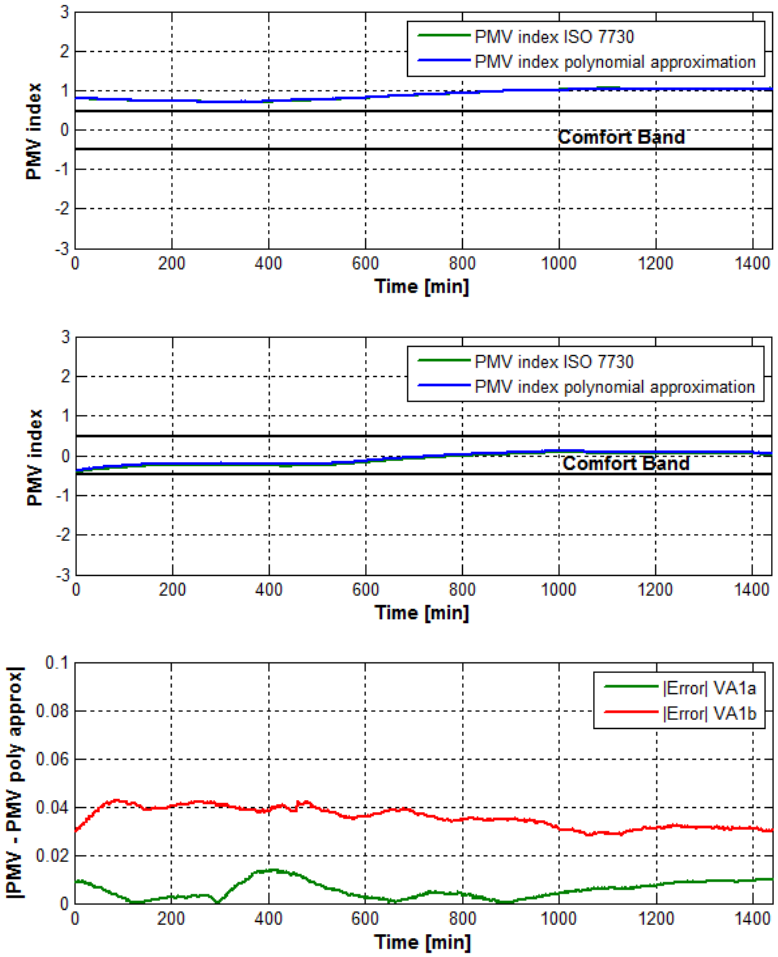

Fig. 3.6 Real PMV index and polynomial approximation for summer data: VA1a (top) and VA1b (middle), and absolute error (real PMV - polynomial approximation) for both data sets (bottom)

With respect to the winter case, the results obtained by the polynomial model for the non-working and working days validation data-sets are $e^{RMS}_{VA2a} = 0.0296$ and $e^{RMS}_{VA2b} = 0.0528$, respectively. The first one, i.e., the results for the non-working day data-set VA2a, are inside the expected range, see top graph at Fig. 3.7. Nevertheless, the results for the working day data-set VA2b, are much worse than expected, see middle graph at Fig. 3.7, with a relative error equal to 10.6%.

Nevertheless, it is important to highlight that, although the polynomial models results are, in general, worse than those obtained from the ANN models, these results are good enough to use the polynomial model to compute the PMV index.

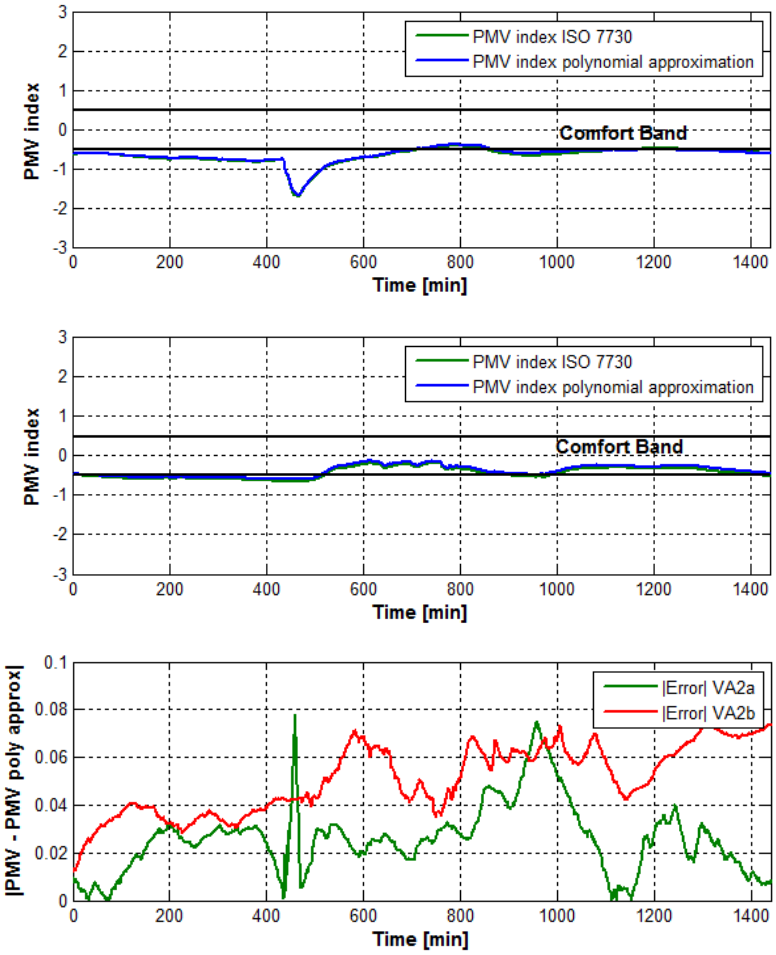

Fig. 3.7 Real PMV index and polynomial approximation for winter data: VA2a (top) and VA2b (middle), and absolute error (real PMV - polynomial approximation) for both data sets (bottom)

To complete this section, a brief comparison between both models based on the RMS error e_S^{RMS} is carried out. First, the error associated with the data-sets for the summer is shown in Table 3.8. As can be observed in that table, the differences between the two summer models are very small. However, the results obtained by the ANN model are better than those obtained by the polynomial model. More specifically, as has previously been commented, this model obtains excellent results with VA1b. However, with the validation data-set for a summer non-working day, VA1a, the obtained results, though good, are worse than those obtained with the polynomial approximation.

Table 3.8 Comparison of summer models using e_S^{RMS} for sets $S \in \{\text{TR1, TE1, VA1a, VA1b}\}$

Model	TR1	TE1	VA1a	VA1b
ANN model with $n_h = 50$	0.0052	0.0051	0.0117	0.0079
Polynomial model order $n = 7$	0.0182	0.0194	0.0065	0.0357

As in the previous case, for the winter case, in each model the errors are very similar for all data-sets: the training set (TR2), the testing set (TE2), the first real validation set for a non-working day (VA2a) and the second real validation set for a working day (VA2b), see Table 3.9.

Table 3.9 Comparison of winter models using e_S^{RMS} for sets $S \in \{\text{TR2, TE2, VA2a, VA2b}\}$

Model	TR2	TE2	VA2a	VA2b
ANN model with $n_h = 50$	0.0175	0.0172	0.0145	0.0123
Polynomial model order $n = 7$	0.0255	0.0266	0.0296	0.0528

It is worth mentioning that, sometimes, the obtained results are not close to the expected ones, as in the case of the polynomial model for the validation data-set VA2b, or the neural network model for the validation data-set VA1b. But, in general, all the obtained results are close to the expected, i.e. RMS errors where about 0.01 and 0.03 are reached for the ANN and polynomial models, respectively. As a conclusion, in the case dealt in this section the ANN model is preferable to the polynomial model since it obtains better results with a similar number of configurable parameters. However, the polynomial model can be used as a good approximation to calculate the PMV index. In addition, although in general the results obtained with the ANN model are better, the polynomial model can be derived in an easier way, hence, it can be linearised around an operation point easily, allowing the implementation of linear controllers for the HVAC system.

3.3.2 Adaptive Indeces

Adaptive indices do not predict the thermal comfort situation, but rather the constant conditions under which people are in a thermal comfort situation inside buildings. Generally, people try to adapt themselves and the surroundings to an ideal thermal condition in order to reduce thermal discomfort. To do that, some conscious actions such as altering clothing, posture, activity levels, rate of work, diet, ventilation, air movement and local temperature are carried taken (ASHRAE, 2009). In addition, an important factor which influences the adaptive process is the outdoor weather conditions and people's exposure to them.

In literature there are several adaptive models which allow the reader to estimate a comfort or neutral temperature as a function of the indoor and outdoor temperatures (Dear et al, 1997; Orosa, 2009). Moreover, the international standard ASHRAE 55 has introduced an adaptive model which depends on the mean outdoor temperature, see Fig. 3.8. This figure, is based on an adaptive model of thermal comfort that is derived from a global database of 21000 measurements taken primarily in office buildings (ASHRAE55, 1992). Therefore, from this figure and according to Eq. 3.14, the indoor operative temperature can be inferred for spaces which satisfy that the metabolic rate associated to the physical activity would be between 1.0 *met* and 1.3 *met*. However, this model cannot be used when outdoor temperature is outside the range $[10^oC, 33.5^oC]$.

$$T_{a_{comf}} = 18.9 + 0.255 T_{a_{out}} \tag{3.14}$$

where $T_{a_{comf}}$ is the comfort temperature and $T_{a_{out}}$ is the outdoor air temperature.

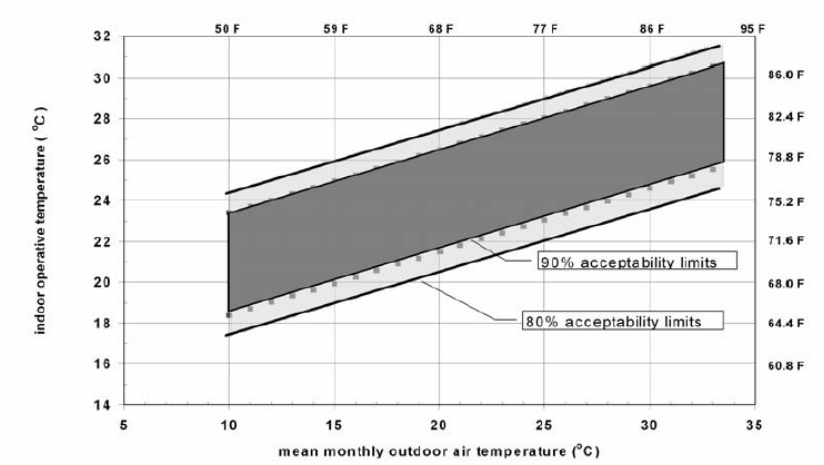

Fig. 3.8 Acceptable operative temperature ranges for naturally conditioned spaces. Source: (ASHRAE55, 1992)

3.3.3 Other Indeces

In this section another couple of indeces which allows the reader to estimate the building's users thermal comfort sensation are presented.

3.3.3.1 Predicted Percent Dissatisfied (PPD)

There is another index very related to the PMV, the Predicted Percentage Dissatisfied (PPD) index. This index reflects the percentage of people that are dissatisfied with the thermal environment (ISO7730, 1994), and it can be estimated according to Eq. 3.15.

$$PPD = 100 - 95\exp\left[-\left(0.03353PMV^4 + 0.2179PMV^2\right)\right] \tag{3.15}$$

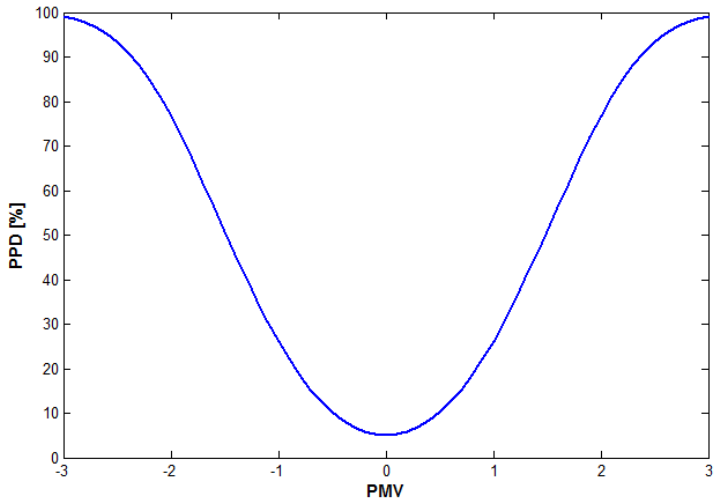

Fig. 3.9 PPD as a function of the PMV

The relationship between PPD and PMV indices can be observed in Fig. 3.9. From this figure, it can be easily deduced that, although an optimal comfort situation will be reached, it is a PMV index equal to zero, it is impossible that 100% of the people will be satisfied with the thermal environment since comfort is a psychological condition, and thus, each person has his own thermal comfort concept. Moreover, for a PMV index equal to zero, approximately 5% of the people are dissatisfied with the thermal environment. The PMV-PPD model is widely accepted in the framework of comfort conditions and it is recognized by international standards as ISO 7730 (ISO7730, 1994).

3.3.3.2 Operative Temperature

Operative temperature can be defined as the average between the mean radiant and indoor air temperatures weighted by their respective heat transfer coefficients, see

Eq. 3.16. Furthermore, for a given value of metabolic rate, clothing insulation, air velocity and humidity, a thermal comfort zone can be defined. More specifically, this comfort zone is defined as a function of the operative temperature ranges which provide acceptable thermal conditions (ASHRAE55, 1992).

$$T_o = \frac{h_r T_{mr} + h_c T_{a_{in}}}{h_r + h_c} \tag{3.16}$$

In the previous equation T_o is the operative temperature $[K]$, T_{mr} and $T_{a_{in}}$ are the mean radiant and indoor air temperatures in $[K]$ respectively, h_c is the convective heat transfer coefficient $[W/m^2K]$, and finally, h_r is the heat transfer coefficient by radiation $[W/m^2K]$.

As an example, in Fig. 3.10 it can be observed that the range of operative temperature associated to winter and summer comfort zones for a rate of people satisfied with the thermal environment equal to 80%, and under these conditions: people inside the environment have activity levels which result in metabolic rates between 1.0 *met* and 1.3 *met*, that is typical office activity levels, the indoor air velocity is lower than 0.2 m/s, and clothing insulation is between 0.5 *clo* (typical summer value) and 1.0 *clo* (winter value). More information about how to use this index under other conditions can be found in (ASHRAE55, 1992)

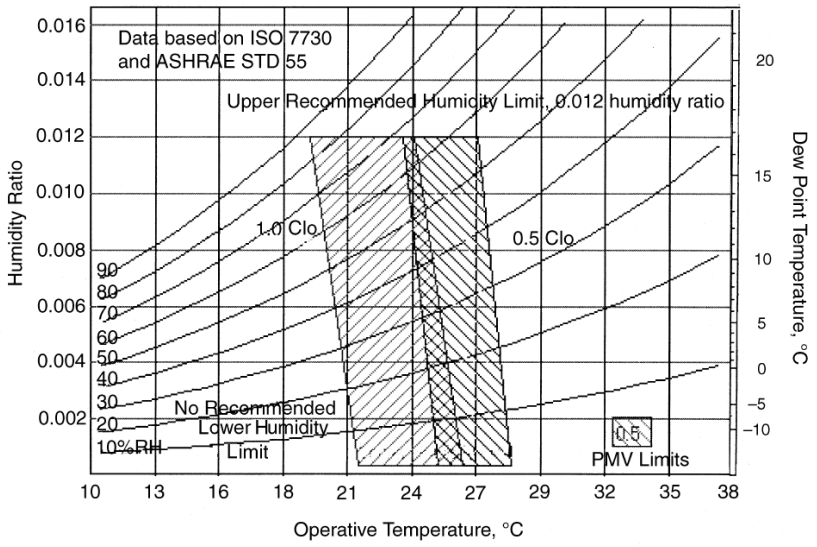

Fig. 3.10 Acceptable range of operative temperature and humidity for spaces that meet the criteria specified in this section. Source: (ASHRAE55, 1992)

3.3.3.3 Givoni Diagrams

These kinds of diagrams, developed by Baruch Givoni, are based on the psychometric diagram, that is, they use air, humidity and temperature main characteristics to evaluate thermal sensation and comfort. Its main objective is to determine the microclimate conditions inside buildings which allow the researchers to evaluate the heating and cooling energy necessary to maintain adequate comfort conditions (Fernández, 1994).

To do that, on the common psychometric diagram, some comfort zones for the winter and the summer are superimposed. The characteristics of these zones can be observed in Table 3.10. In addition, a scheme is also included which contains the main strategies which will be necessary to apply in order to correct the behaviour of the building, that is, to translate a data point from outside to the comfort zone (Givoni, 1994). As an example, if most parts of the points fall into the *E* zone, the recommended strategy will be to turn on the ventilation in order to move these points into the comfort zone, see Fig. 3.11.

Table 3.10 Comfort zones inside the psychometric diagram

Parameter	Summer	Winter
Indoor air temperature [^{o}C]	23-26	20-24
Relative humidity [%]	40-60	40-60

3.4 Visual Comfort Indeces

In general, most works which can be found in literature try to reach an optimal visual comfort situation by maintaining the illumination level inside the recommendations provided by international standards. However, as was mentioned in Sect. 3.2.2, visual comfort conditions depend on several factors, such as, illumination level, glare and colour rendering. In this section, each of the previous parameters is going to be analysed and some indeces to estimate them are provided.

3.4.1 Illumination Level

One of the main parameters which influence visual comfort is the illumination level. It is established by international standards (12665, 2002; 12464-1, 2002) as a function of the type of environment (offices, schools, hospitals, etc.) and the performed activity inside it. The most energy efficient way of obtaining these optimal illumina-

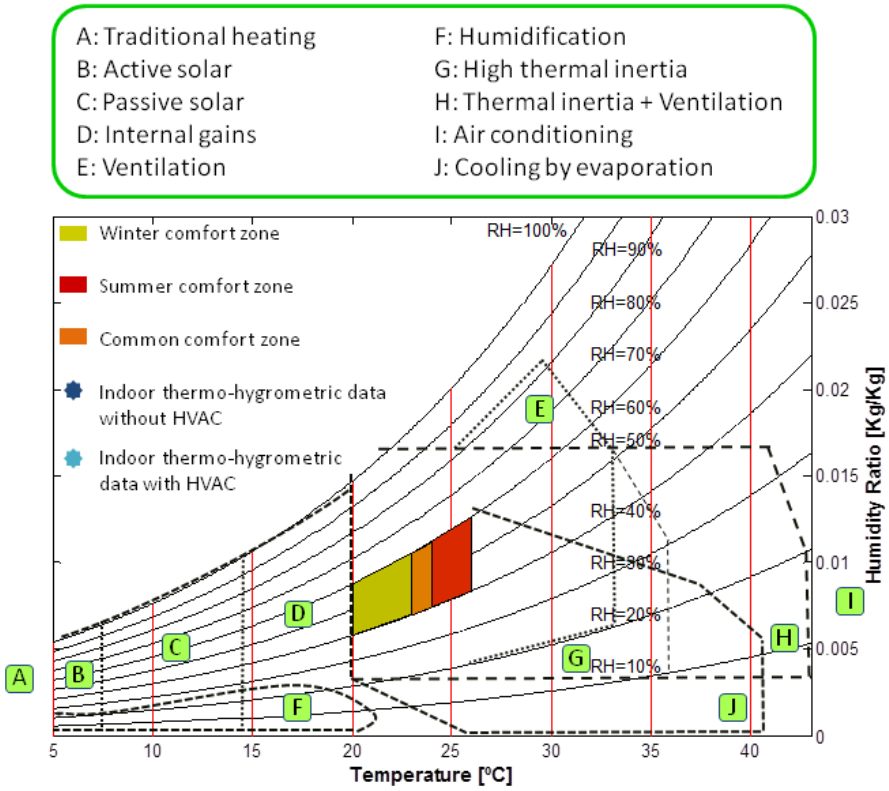

Fig. 3.11 Example of Givoni diagram

tion levels inside a certain environment is through the use of daylight. Therefore, the illumination level provided by daylight will depend on some physical properties of the environment such as the number, design and orientation of windows, light reflection coefficients, etc. (Koçlar et al, 2004). Nevertheless, sometimes it is not possible to reach the optimal illumination level using only daylight, thus, it is necessary to use some artificial lighting mechanism (Kim, 2010).

To evaluate the illumination level inside a certain environment, in Castilla et al (2010a) an index called D_i, which represents the difference between the optimal and the real illumination levels, was proposed, see Eq. 3.17.

$$D_i = E_{vd} - E_{vr} \tag{3.17}$$

where E_{vd} and E_{vr} are the optimal and real illumination levels in $[lux]$.

3.4.2 Glare

According to (CIBSE, 2002), glare can be defined as that *"condition of vision in which there is discomfort or a reduction in the ability to see details or objects, caused by an unsuitable distribution or range luminance, or to extreme contrasts"*. Although there are many indeces for visual discomfort due to glare in literature, the most extended ones are the Unified Glare Rating (UGR) index and the Daylight Glare Index (DGI).

3.4.2.1 Unified Glare Rating (UGR) Index

The UGR index expresses the discomfort glare occasioned by the presence of bright light sources, luminaries or windows (CIBSE, 2009). It can be estimated according to Eq. 3.18. UGR index values are within the range of 13 to 30, and moreover, the lower UGR values, the less visual discomfort condition.

$$UGR = 8\log_{10}\frac{0.25}{L_b}\sum_{i=1}^{N}\frac{L_{s_i}^2\omega_i}{p_{Guth_i}^2} \tag{3.18}$$

where L_b is the background luminance in $[cd/m^2]$, N represents the number of luminaries inside the room, and L_{s_i}, ω_i and p_{Guth_i} are the luminance in $[cd/m^2]$, the solid angle subtended at the observer's eye and the Guth position index provided by the i^{th} luminary, respectively.

The Guth position index, p_{Guth}, was proposed by Luckiest and Guth (1949) in 1949 and reflects the relative Borderline between Comfort and Discomfort (BCD) brightness of a luminary displaced from the line of vision in terms of the BCD brightness of a luminary located on the line of vision. This index was developed as a function on the experiments performed with 50 subjects aged from 20 to 40. The methodology used to determine this index is briefly explained in Kim and Kim (2010).

3.4.2.2 Discomfort Glare Index (DGI)

This index is employed to evaluate the daylight discomfort glare for light sources with non-uniform levels of luminance (Bellia et al, 2008). It can be estimated according to Eq. 3.19.

$$DGI = 10\log_{10}\sum_{i=1}^{N}0.478\left[\frac{L_{s_i}^{1.6}\omega_i^{0.8}}{L_b + (0.07\omega_w^{0.5}L_w)}\right] \tag{3.19}$$

In the previous equation N is the number of luminaries inside the room, L_{s_i} is the luminance provided by the i^{th} luminary in $[cd/m^2]$, ω_w is the solid angle of the

window, L_w is the weighted average luminance of the window in $[cd/m^2]$ and ω_i is the solid angle of the i^{th} luminary.

3.4.3 Colour Rendering

Finally, another important factor for visual comfort conditions is related to the natural rendering of the objects and human skin colour inside an environment, that is, it represents the ability of a light source to show the colours of the objects and human skin naturally in comparison with a reference light source. In order to obtain a quantitative measure of the colour rendering associated to a light source, the general colour-rendering index has been proposed.

The maximum value of this index is 100, and it decreases with decreasing colour-rendering quality (CIBSE, 2002). Furthermore, light sources with a colour-rendering index lower than 80 should not be used in indoor environments where people remain for long periods of time (CIBSE, 2002).

3.5 Indoor Air Quality Indeces

3.5.1 Indoor Air Quality (IAQ) index

Most of the works which can be found in literature use direct CO_2 concentration in order to reach indoor air quality. Within the scope of this book a new index is proposed: the Indoor Air Quality (IAQ) index. This index classifies indoor air for occupied rooms, where smoking is not allowed and pollution is caused mainly by human metabolism, according to the four indoor-air quality categories presented in Table 3.3. IAQ index is estimated based on indoor CO_2 concentration and the classification provided by the international standard prEn-13779 (prEN 13779, 2007), see Eq. 3.20. More specifically, it has been considered an optimal indoor air quality for CO_2 level under 500 ppm, and thus, the IAQ index is less than or equal to zero. After that, for a higher CO_2 level, the IAQ index increases following a linear regression, see Eq. 3.20.

$$IAQ = 0.001 CO_{2_{in}} - 0.5 \tag{3.20}$$

The result provided by this index is evaluated through a four-point indoor-air quality sensation scale, see Table 3.11. Hence, to guarantee indoor air quality in a certain environment, it is recommended to maintain a CO_2 concentration level between 500 ppm and 600 ppm (Berenguer and Bernal, 1994), that is an IAQ index value at 0 with a tolerance of 0.1.

Table 3.11 Indoor air quality sensation scale

IAQ	Sensation
$IAQ \leq 0$	High indoor air quality (IDA-1)
$0 < IAQ < 0.1$	Medium indoor air quality (IDA-2)
$0.1 \leq IAQ < 0.5$	Moderate indoor air quality (IDA-3)
$0.5 \leq IAQ \leq 1$	Low indoor air quality (IDA-4)

3.6 Comfort Analysis

As was pointed out previously, in this section an analysis of the users' comfort inside a characteristic room of the CDdI-CIESOL-ARFRISOL building is presented. In Castilla et al (2010b) a complete comfort analysis of most representative environments of this building can be found. The main objective of this study is to evaluate the performance of the passive bioclimatic strategies presented within Chap. 2 without the use of any control strategy. To do that, measured data from 2009 and 2010 have been used. More specifically, comfort analysis was performed along three different periods of the year, the summer, the winter and an in-between period, the autumn. For each of the periods approximately fifteen days have been analysed: from the 1^{st} (Saturday) to the 15^{th} (Saturday) of August, 2009 for the summer period, from the 13^{th} (Saturday) to the 24^{th} (Wednesday) of February, 2010 for the winter period, and from the 1^{st} (Sunday) to the 15^{th} (Sunday) of November, 2009 for the autumn. Besides that, as the building does not have a fixed work schedule, the following assumptions have been established:

- Saturdays and Sundays are considered periods of non-occupation, that is, the building is supposed to be empty.
- Within the occupation periods (from Monday to Friday) a night time period that extends from 21:00 PM to 07:00 AM is established.

3.6.1 Thermal Comfort Analysis by Means of PMV and PPD Indices

First of all, a thermal comfort analysis based on PMV and PPD indices has been performed. For each of the studied periods (summer, winter and autumn) a figure is included. Within these figures, the results are organized as follows: the top picture shows the evolution of the PMV index along the studied period (approximately 15 days), in the middle picture the evolution of the PPD index can be observed, and finally, at the bottom picture the energy extracted or added to the analysed environment is displayed.

Furthermore, this energy is estimated as a function of the heat exchange that happens in the analysed environment by means of the HVAC system, see Eq. 3.21.

$$E_{HVAC} = \rho_W q_W C_p \Delta T \tag{3.21}$$

where ρ_W is the water density in $[kg/m^3]$, q_W is the water flow rate in the fancoil unit $[m^3/s]$, C_p is the specific heat in $[J/(kgK)]$, and ΔT is the difference between impulse and return fancoil air temperatures in $[K]$.

According to the Papadakis classification (Papadakis et al, 1966), Almería has a subtropical semidesert Mediterranean climate with an annual average number of 2965 hours of sunshine and a mean annual number of 26 precipitation days (climate values registered at the meteorologic station of the Almería airport, situated 3.5 *km* away from the building), see Table 3.12, and thus, it is characterized by having hot summers and cool to mild winters. More specifically, during the warmest months the average maximum and minimum temperatures are equal to 30.7 ^oC and 22 ^oC, respectively. Furthermore, during the winter period, daily maximum and minimum mean air temperatures are equal to 22 ^oC and 8.8 ^oC, respectively.

Table 3.12 Climate data for Almería (climate values registered at the meteorologic station of Almería airport, situated 3.5 *km* from the building)

Parameter	Summer period	Winter period	Autumn period
Maximum mean air temperature $[^oC]$	30.7	17.7	20.4
Minimum mean air temperature $[^oC]$	22	8.8	12.0
Mean relative humidity $[\%]$	65	68	70
Average precipitation days $[-]$	0	3	3
Mean monthly sunshine hours $[-]$	312	191	187

- The summer period. As shown in the top picture of Fig. 3.12, there are some days in which the PMV index is outside the comfort zone and other days where this index is inside the comfort zone. Moreover, if the top picture is compared to the bottom graph, it can be observed that there is an increment in energy consumption those days in which the PMV index is located inside the comfort zone. From this, it can be inferred that the environment was occupied and besides the HVAC system was working. Finally, in the middle figure it is shown that although the PMV index was equal to zero, there is a percentage of people approximately equal to 5% which is dissatisfied with the thermal environment. Furthermore, when the room is closed for a long time (3-4 consecutive days) this PPD increases nearly 80% mainly due to the lack of ventilation and refrigeration.
- The winter period. The obtained results derived from the thermal comfort analysis for the winter period are shown in Fig. 3.13. As can be observed in the top graph of this figure, most of the time the PMV index is below the comfort zone. In addition, these periods in which PMV is located inside the comfort zone are associated to the use of the heating system, see bottom picture in 3.13 where a

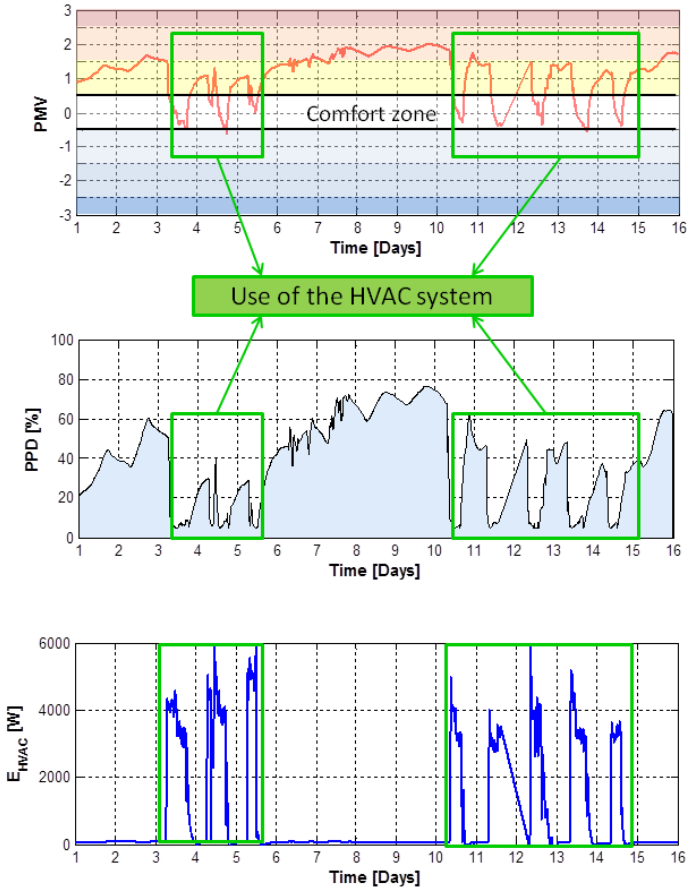

Fig. 3.12 Thermal comfort analysis for the summer period: the PMV index (top), the PPD index (middle) and energy consumption (bottom)

considerable increment of the energy consumption can be observed at several periods of time. Moreover, from the middle picture it can be inferred that the PPD index is inferior to than 10% along these periods of time in which the heating system is working.

- The autumn period. Figure 3.14 shows the results derived from the thermal comfort analysis along the autumn period with the PMV and PPD indices. As can be seen in the top picture of this figure, most of the time the PMV index is inside the comfort zone. However, the 14^{th} of November was a cold day and it was necessary to use the heating system in order to achieve the appropriate thermal conditions. This hypothesis can be confirmed by means of the bottom graph in Fig. 3.14, where a considerable increment of energy consumption can be ob-

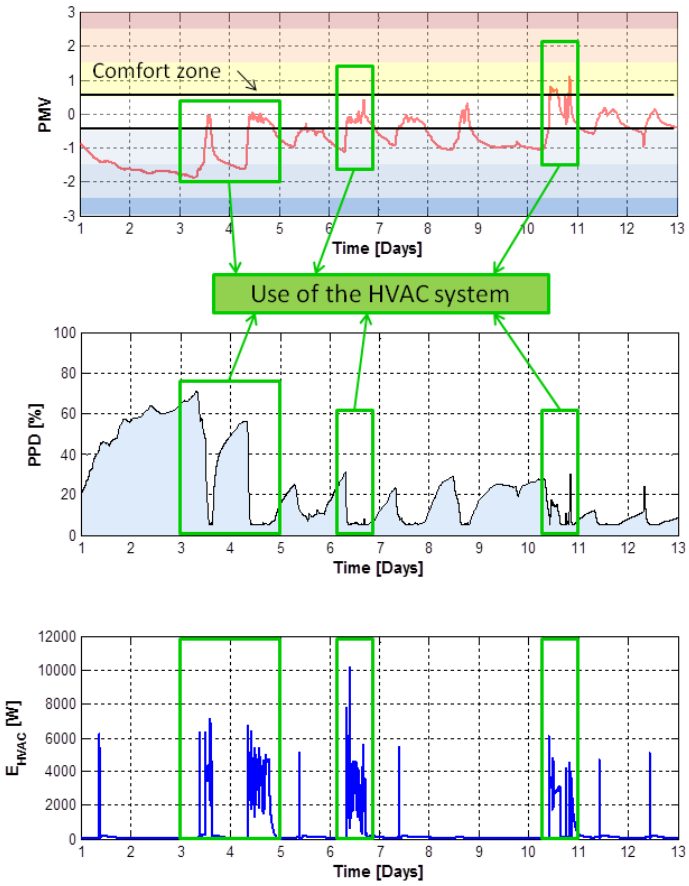

Fig. 3.13 Thermal comfort analysis for the winter period: the PMV index (top), the PPD index (middle) and energy consumption (bottom)

served. Finally, in the middle picture, the PPD index is less than 20% along the whole period is shown.

3.6.2 Thermal comfort analysis by means of Givoni diagrams

As in the previous thermal comfort analysis, Givoni diagrams have been obtained for three different periods of the year, the summer, the winter and an in-between period, the autumn. More specifically, Fig. 3.15 shows the summer period, in Fig. 3.16 the results obtained for the winter period are shown, and finally, the results derived from the autumn can be observed in Fig. 3.17.

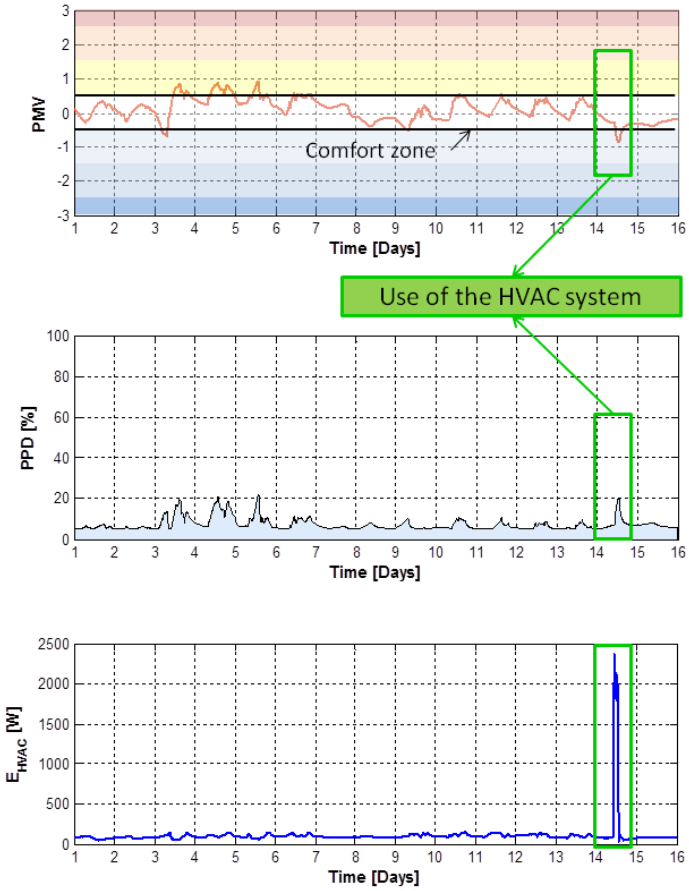

Fig. 3.14 Thermal comfort analysis for an in-between period (the autumn): the PMV index (top), the PPD index (middle) and energy consumption (bottom)

For the summer period, see Fig. 3.15, it can be observed, without taking into account the state of the HVAC system, that most of the data points are located outside the comfort zone defined for the summer, and besides, the strategies that are necessary to apply in order to correct this behaviour will be a combination between air conditioning and thermal inertia plus ventilation. However, taking into account the real state of the HVAC system (on/off), a detailed analysis has been performed. More specifically, the total thermo-hygrometric data set has been divided into two smaller data sets which represent both the thermo-hygrometric data with the HVAC turned on (light blue) and turned off (dark blue). To do that, the energy extracted or added to the room, which can be observed in the bottom picture of Fig. 3.12, has been used. Moreover, as shown in the enlargement of the comfort zone included in Fig. 3.15, at first, when the HVAC was turned off for a considerable time period,

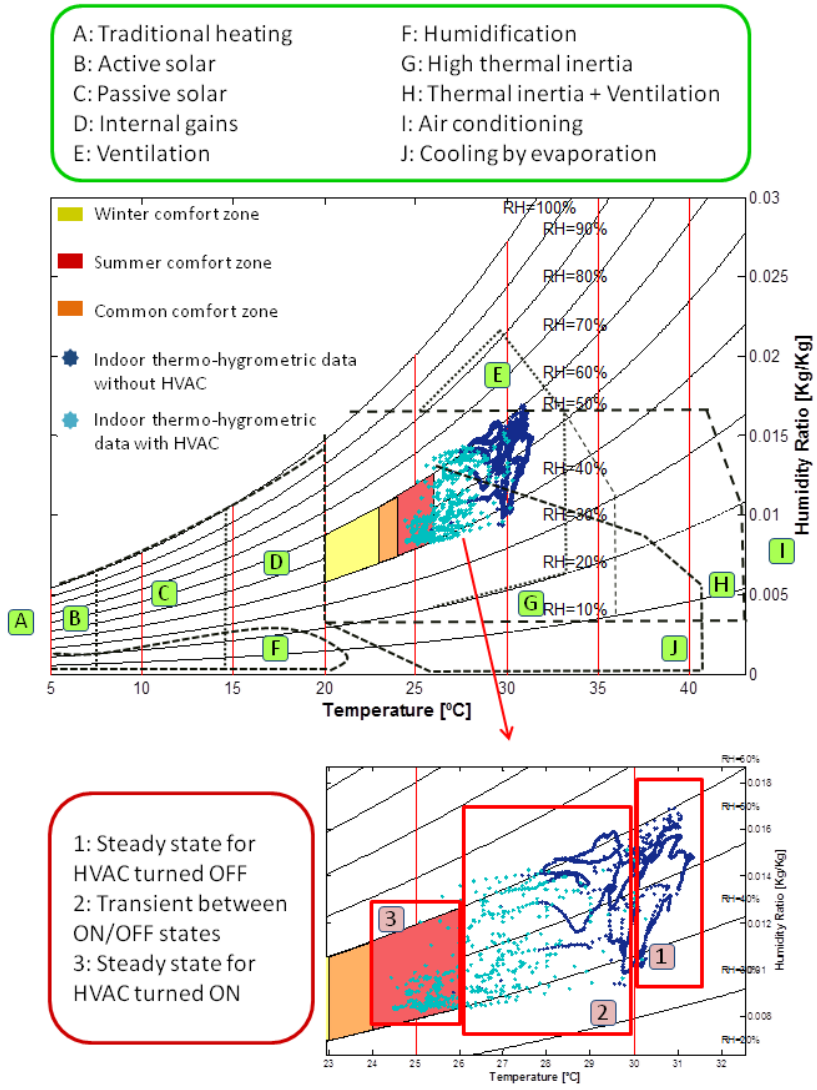

Fig. 3.15 Givoni diagram for the summer period

the room is in a stationary state and the thermo-hygrometric data is totally located outside of the comfort zone (see the red rectangle labelled number one), then, when the HVAC is turned on, the room begins to cool down and the thermo-higrometric data is displaced towards the comfort zone (see the red rectangle labelled number

two). Finally, once the HVAC has been turned on for a certain period of time, and the room is totally cooled, a stationary state which is within the comfort zone is reached (see the red rectangle labelled number three). Furthermore, when the HVAC is disconnected the inverse process happens, that is, the thermo-hygrometric data changes from the red rectangle labelled number three to the one labelled number one.

On the other hand, as shown in Fig. 3.16 for the winter period there is also a large amount of data outside the defined comfort zone, thus the strategies which are necessary to apply in order to correct this behaviour are internal gains and thermal inertia combined with ventilation. In addition, in this case, an analysis of the thermo-hygrometric data as a function of the real state of the HVAC has also been performed. The results derived from it can be observed in the expanded view of the comfort zone included in Fig. 3.16, and basically, they demonstrate that the system behaves in a similar way as the summer period. However, if the red rectangle labelled number three is observed, it can be inferred that there is a certain data set outside the comfort zone due to an excess of temperature caused by an excessive use of the HVAC. The main reason for this behaviour is that, at this time, a manual HVAC control was installed, that is, the users of the room could decide when the HVAC had to be turned on and off. Therefore, sometimes they were not able to regulate it in an appropriate way which is related both directly to the lack of comfort for the users, and indirectly to an unnecessary energy consumption.

Finally, for the autumn period, which is shown in Fig. 3.17, there is a considerable amount of data points inside the comfort zone. However, there is another set of data points which is outside the comfort zone and to correct this behaviour it should be necessary to apply high thermal inertia strategies and even ventilation. In addition, and as a difference with respect to the summer and the winter periods, during this period the HVAC is turned off most of the time.

3.6.3 Indoor Air Quality Analysis by Means of IAQ Index

Lastly, an analysis of the indoor air quality inside the characteristic room of the CDdI-CIESOL-ARFRISOL building has been performed. To do that, the proposed IAQ index, see Sect. 3.5.1, has been used. Moreover, and as in the previous analysis, three different periods have been analysed, the summer, the winter and the autumn. The obtained results, see Fig. 3.18, show that when the room is empty there is a high indoor air quality (IDA-1). This is because the IAQ index depends exclusively on the CO_2 concentration, which is the main waste from people's presence. Therefore, when the IAQ index is out of the associated IDA-1 zone it indicates the presence of humans in the room.

In addition, from the obtained results the influence of the HVAC system in order to maintain indoor air quality can be inferred. More specifically, if the IAQ index results are compared to the bottom picture of Figs. 3.12 (for the summer), 3.13 (for the winter) and 3.14 (for the autumn), that is, when the HVAC system is being used, it can be observed that the use of the HVAC helps to improve indoor air quality from

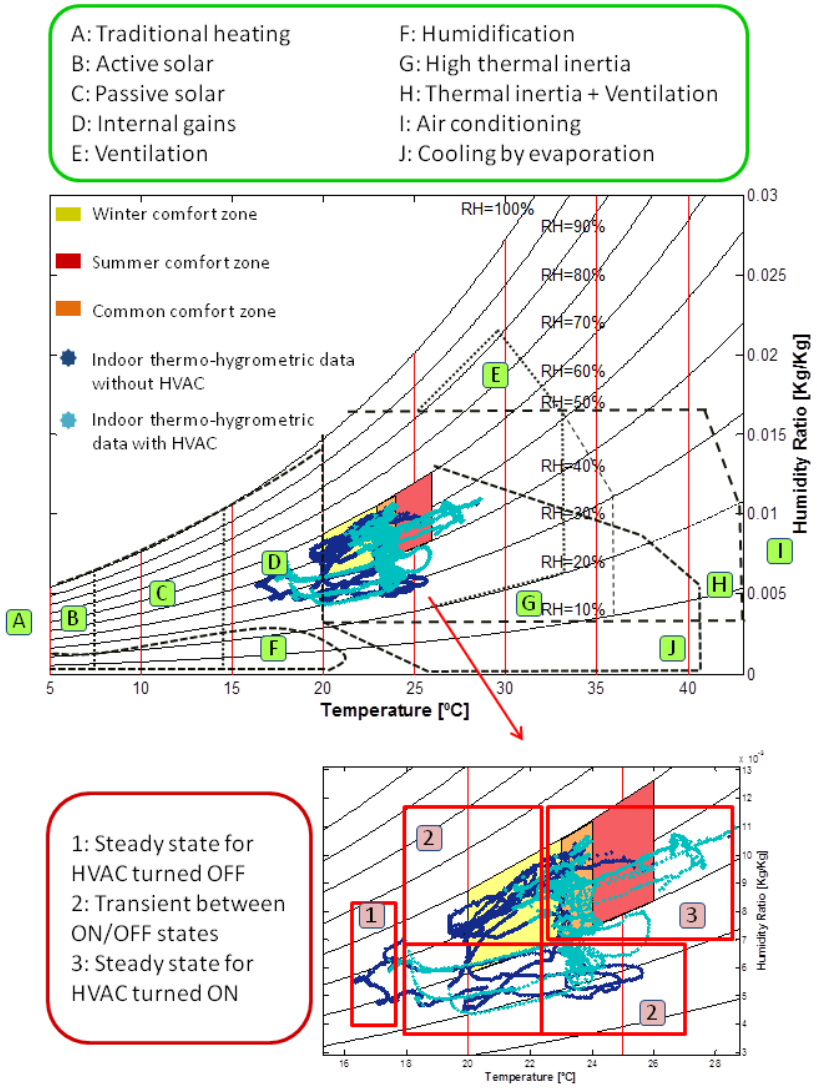

Fig. 3.16 Givoni diagram for the winter period

IDA-4 or IDA-3 to IDA-2 or even IDA-1 as a function of the number of people inside the room. However, in some cases, for example if there are a lot of people inside the room, it is necessary to use another strategy to reduce CO_2 concentration to levels inside the IDA-1 zone. This strategy can be the use of natural ventilation through the

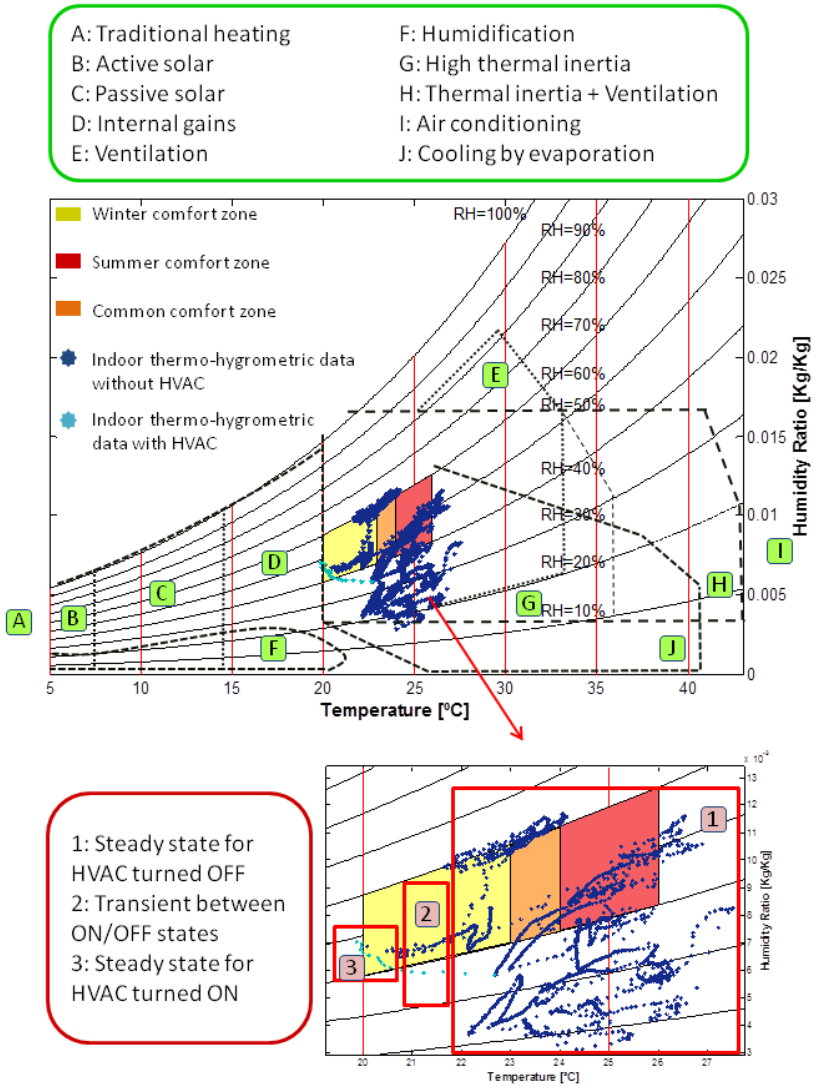

Fig. 3.17 Givoni diagram for an in-between period (the autumn)

windows. Nevertheless, the use of it also has a direct influence on thermal comfort. Hence it is necessary to look for a tradeoff between thermal comfort and indoor air quality.

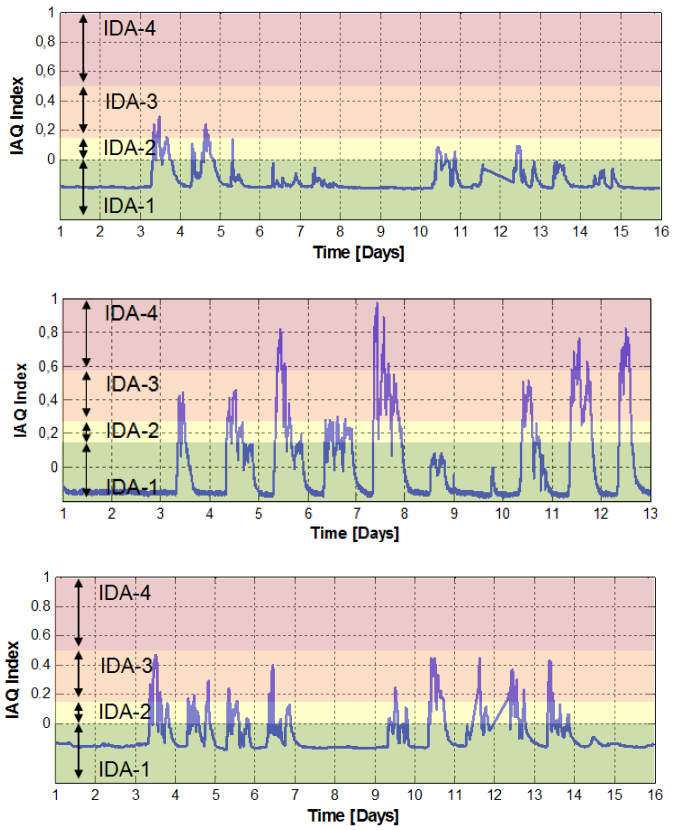

Fig. 3.18 Evolution of the IAQ index for the summer (top), the winter (middle) and the autumn (bottom) periods

3.6.4 Main Conclusions of the Comfort Analysis

The main conclusions which can be inferred from the comfort analysis performed in this section are that the obtained results for both summer and winter periods are similar, making the use of an HVAC system to cool in summer, and to heat in winter necessary. In addition, and according to the results of the in-between period, the autumn, it has been demonstrated that along most part of these periods, the passive strategies of the building allow its users to reach a comfort situation inside it without using any active strategy. However, the existence of a significant percentage of data outside the comfort zone during the summer and the winter periods makes necessary to consider two hypothesis which are not strictly exclusive:

- Insufficient of manual control that was implemented in the HVAC system.

- Existence of subjective factors in the evaluation of both thermal comfort and indoor air quality.

In addition, both circumstances have, at the same time, consequences in the energy consumption derived from the actuators since the inadequate operation of these systems, as well as, their use out of their operation points cause performance and durability losses. Hence, as a function of the comfort analysis that has been widely commented in this section, it is necessary to develop a specific control system which allows the users to maintain environmental conditions of the building inside a comfort zone for the user minimising, at the same time, energy consumption.

Therefore, the idea is to develop a hierarchical control architecture able to generate, in the higher layer, the appropriate setpoints necessary to reach an optimal comfort situation, and to develop some control algorithms in the lower layer that act on control variables.

To do that, several environments of the CDdI-CIESOL-ARFRISOL building were set up by means of the installation of different actuators and new sensors as was described in Chap. 2. More specifically, motors which allow the automatic aperture/closure of the windows in order to regulate the indoor air flow, motors for the blinds that were used to regulate the amount of heat that flows through the glass of the windows were installed, etc. Therefore, the control system has as control variables the fancoil and both the aperture degree of windows and blinds, and as output variables ideal thermal comfort and indoor air quality conditions. This is not a trivial problem, since the system contains several disturbances such as the number of people, the outdoor climate conditions, the relative humidity, etc. In the following chapters, several solutions adopted to solve this problem are shown.

3.7 Conclusions

Most of the time, people develop their routine inside a building environment, thus it is important that the environment where they usually spend time has optimal conditions for them, that is, it should be comfortable. Hence, in this chapter a definition of a comfort situation has been given considering two important factors: thermal comfort and indoor air quality. Moreover, several ways of estimating them have been proposed. In addition, a comfort analysis for a room of the CDdI-CIESOL-ARFRISOL building based on some of the indices presented in this chapter has been performed. From this analysis, it can be deduced that comfort cannot be considered a constant and general factor and to reach it, outdoor environmental conditions have to also be taken into account.

Finally, as a conclusion, it has been decided that it is necessary to develop a specific control system that allows the building's users to obtain a high comfort level minimising, at the same time, energy consumption. To do that, a selection among the explained comfort indices has been performed. More specifically, in order to control thermal comfort the PMV index has been selected since it is one of the most used indices and it is widely recognized by international standards. In addition, as

mentioned throughout this chapter, it takes into account not only indoor air temperature and relative humidity, but also indoor air velocity and the physical activity performed by people. Furthermore, to control the indoor air quality, the proposed IAQ index will be used.

References

12464-1 E (2002) Light and lighting - Lighting of work places - Part 1: indoor work places. Brussels: European Commitee for Standardization

12665 E (2002) Light and lighting - Basic terms and criteria for specifying lighting requirements. Brussels: European Commitee for Standardization

ASHRAE (2009) ASHRAE Handbook - Fundamentals. Refrigerating American Society of Heating and Air-Conditioning Engineers

ASHRAE55 (1992) Thermal environment conditions for human occupancy. American Society of Heating Ventilating and Air-conditioning Engineers

Atthajariyakul S, Leephakpreeda T (2004) Real-time determination of optimal indoor-air condition for thermal comfort, air quality and efficient energy usage. Energy and Buildings 36:720–733

Atthajariyakul S, Leephakpreeda T (2005) Neural computing thermal comfort index for HVAC systems. Energy Conversion and Management 46:2553–2565

Awbi HB (2003) Ventilation of Buildings. Spon Press

Bedford T, Warmer CG (1934) The globe thermometer in studies of heating and ventilation. Journal of Hygiene 34:458–473

Bellia L, Cesarano A, Iuliano GF, Spada G (2008) Daylight glare: A review of discomfort indexes. In: Proceedings of Visual Quality and Energy Efficiency in Indoor Lighting: Today for Tomorrow, Rome, Italy

Berenguer MJ, Bernal F (1994) NTP 549: Carbon dioxide in the evaluation of Indoor Air Quality (in Spanish). Tech. rep., Instituto Nacional de Seguridad e Higiene en el Trabajo. Ministerio de Trabajo y Asunstos Sociales

Castilla M, Álvarez JD, Berenguel M, Pérez M, Guzmán JL, Rodríguez F (2010a) Comfort optimization in a solar energy research center. In: IFAC Conference on Control Methodologies and Technology for Energy Efficiency, Vilamoura, Portugal

Castilla M, Ferre JA, Pérez M, Jiménez MJ, Álvarez JD, Berenguel M (2010b) Análisis experimental del CDdI del SP2 CIESOL en la Universidad de Almería. Estudio de confort. Datos preliminares de Agosto de 2009 a Enero de 2010. (in Spanish). Tech. rep., Universidad de Almería

Castilla M, Álvarez JD, Ortega MG, Arahal MR (2013) Neural network and polynomial approximated thermal comfort models for HVAC systems. Building and Environment 59:107–115

CIBSE (2002) Code for Lighting. The Society of Light and Lighting

CIBSE (2009) The SLL Lighting Handbook. The Society of Light and Lighting

Cybenko G (1989) Approximation by superpositions of a sigmoidal function. Mathematics of Control, Signals, and Systems 2:303–314

Dear R, Brager G, Cooper D (1997) Developing an adaptive model of thermal comfort and preference. Final Report ASHRAE RP-884

D'Errico J (2012) Polyfitn. http://www.mathworks.com/matlabcentral/fileexchange/34765-polyfitn, Last access 19th February 2013

Dounis AI, Caraiscos C (2009) Advanced control systems engineering for energy and comfort management in a building environment - a review. Renewable and Sustainable Energy Reviews 13:1246–1261

Fanger PO (1972) Thermal comfort analysis and applications in environment engeering. McGraw Hill

Fanger PO (1973) Assessment of man's thermal comfort in practice. British Journal of Industrial Medicine 30(4):313–324

Fernández F (1994) Clima y confortabilidad humana. aspectos metodológicos (in Spanish). Serie geográfica 4:109–125

Frontczak M, Wargocki P (2011) Literature survey on how different factors influence human comfort in indoor environments. Building and Environment 46:922–937

Givoni B (1994) Passive and low energy cooling of buildings. John Wiley & Sons

Guasch J, Forster R, Ramos F, Hernández A, Smith NA (2001) Enciclopedia de salud y seguridad en el trabajo: Iluminación (in Spanish). Tech. rep., Organización Internacional del Trabajo. Ministerio de Trabajo y Asuntos Sociales

Hernández A (1994) NTP 343: Nuevos criterios para futuros estándares de ventilación de interiores (in Spanish). Instituto Nacional de Seguridad e Higiene en el Trabajo Ministerio de Trabajo y Asuntos Sociales, Spain

Homoda RZ, Saharia KSM, Almuribb HAF, Nagi FH (2012) RLF and TS fuzzy model identification of indoor thermal comfort based on PMV-PPD. Building and Environment 49:141–153

Huang GB, Chen YQ, Babri H (2000) Classification ability of single hidden layer feedforward neural networks. IEEE Transactions on neural networks 11(3):799–801

IDAE (2007) Reglamento de instalaciones térmicas en los edificios. Tech. rep., Ministerio de Industria, Turismo y Comercio

ISO7730 (1994) Moderate thermal environments. Determination of the PMV and PPD indices and specification of the conditions for thermal comfort. International Organisation for Standardisation

Kim G J T andd Kim (2010) Overview and new developments in optical daylighting systems for building a healthy indoor environment. Building and Environment 45:256–269

Kim W, Kim JT (2010) A formula of the position index of a glare source in the visual field. In: 3rd International Symposium on Sustainable Healthy Buildings, SHB2010, Seoul, Korea

Koçlar G, Köknel A, Tamer N (2004) Building envelope design with the objective to ensure thermal, visual and acoustic comfort conditions. Building and Environment 39(3):281–287

Kolokotsa D, Tsiavos D, Stavrakakis GS, Kalaitzakis K, Antonidakis E (2001) Advanced fuzzy logic controllers design and evaluation for buildings' occupant thermal-visual comfort and indoor air quality satisfaction. Energy and Buildings 33:531–543

Liang J, Ruxu D (2005) Thermal comfort control based on neural network for HVAC application. In: Proceedings of the 2005 IEEE Conference on Control Applications, Toronto, Canada, pp 819–824

Liu W, Lian Z, Zhao B (2007) A neural network evaluation model for individual thermal comfort. Energy and Buildings 39:1115–1122

Luckiest M, Guth SK (1949) Brightnesses in visual field at Borderline between Comfort and Discomfort (BCD). Illuminating Engineering 44:650–670

Moré JJ (1978) Numerical Analysis. Lecture Notes in Mathematics, vol 630, Springer, chap The Levenberg-Marquardt algorithm: Implementation and theory, pp 105–116

Orosa JA (2009) Research on general thermal comfort models. European Journal of Scientific Research 27(2):217–227

Papadakis J, et al (1966) Climates of the world and their agricultural potentialities. Climates of the world and their agricultural potentialities

prEN 13779 (2007) Ventilation for non-residential buildings - Performance requirements for ventilation and room-conditioning systems. European Committee for Standardization

prEN 15251 (2007) Indoor environmental input parameters for design and assessment of energy performance of buildings addressing indoor air quality, thermal environment, lighting and acoustics. European Committee for Standardization

Reed RD, Marks RJ (1999) Neural smithing. Supervised learning in feedforward artificial neural networks. The MIT Press

Ruano AE, Crispim EM, Conceiçao EZE, Lúcio MMJR (2006) Prediction of building's temperature using neural networks models. Energy and Buildings 38:682–694

Sherman M (1985) A simplified model of thermal comfort. Energy and Buildings 8(1):37–50

Taleghani M, Tenpierik M, Kurvers S, Dobbelsteen A (2013) A review into thermal comfort in buildings. Renewable and Sustainable Energy Reviews 26:201–215

Tse WL, Chan WL (2008) A distributed sensor network for measurement of human thermal comfort feelings. Sensors and Actuators A: Physical 144(2):394–402

Van Hoof J (2008) Forty years of Fanger's model of thermal comfort: comfort for all? Indoor Air 18(3):182–201

Vernon HM (1932) The globe thermometer. Proceedings of the Institution of Heating and Ventilating Engineers 39:100–104

Wan JW, Yang K, Zhang WJ, Zhang JL (2009) A new method of determination of indoor temperature and relative humidity with consideration of human thermal comfort. Building and Environment 44(2):411–417